Research Article

Hongkai Zhao*, Dengchao Zhang*, and Yingshuang Li

Morphology and crystallization kinetics of Rubber-modified Nylon 6 Prepared by Anionic In-situ Polymerization

https://doi.org/10.1515/secm-2020-0020
Received Jan 25, 2020; accepted May 03, 2020

Abstract: In this work, we modified nylon 6 with liquid rubber by in-situ polymerization. The infrared analysis suggested that HDI urea diketone is successfully blocked by caprolactam after grafting on hydroxyl of HTPB, and the rubber-modified nylon copolymer is generated by the anionic polymerization. The impact section analysis indicated the rubber-modified nylon 6 resin exhibited an alpha crystal form. With an increase in the rubber content, nylon 6 was more likely to generate stable α crystal. Avrami equation was a good description of the non-isothermal crystallization kinetics of nylon-6 and rubber-modified nylon-6 resin. Moreover, it is found that the initial crystallization temperature of nylon-6 chain segment decreased due to the flexible rubber chain segment. n value of rubber-modified nylon-6 indicated that its growth was the coexistence of two-dimensional discoid and three-dimensional spherulite growth. Finally, the addition of the rubber accelerated the crystallization rate of nylon 6.

Keywords: Nylon 6; In-situ polymerization; Liquid ubber; Morphological structure; Crystallization kinetics

1 Introduction

Nylon 6 (PA6), which has high strength, wear resistance, oil resistance, weak acid and alkali resistance and good toughness, is widely used in the industrial field. However, it has disadvantage of low impact strength at dry state and low temperature. The rubber is used for grafting the active functional group, and blending with nylon 6, such as ethylene-propylene methylene copolymer (EPM)/salicylic acid grafting ethylene-propylene methylene copolymer (EPM-g-SA)/nylon 6 [1, 2], ethylene-propylene-diene monomer (EPDM)/nylon 6 [3], nylon 6/ethylene-propylene rubber (EPR) [4, 5], nylon 6/methyl acrylate grafting hydrogenated styrene-butadiene block copolymer (SEBS-g-MA) [6] and nylon 6/acrylic rubber (AR) [7]. Their performances have been improved to a certain extent, but the compatibility of the two components is limited. The phase separation becomes serious as the modified ingredients are increased, so, the mechanical properties of blends cannot be improved synergistically. Nylon 6 modified by in-situ polymerization shows better performance than that of blending, filling and other methods. The modified nylon 6 resin with high performance is prepared by random and block copolymerization or graft polymerization. Currently, the elastomer or rubber is often used to modify nylon 6 by anionic polymerization with it. The modified resin has the excellent comprehensive performance, such as low price and good processability. Generally, the elastomer can be polydimethylsiloxane [8], lactone [9–11], polyurea [12], poly-oxypropylene [13], polyethylene glycol (PEG) [14, 15], tetrahydrofuran [16], and other forms of polyether [17]. The rubber prepolymer is used for modifying nylon 6 resin, such as amino-terminated liquid nitrile rubber (ATBN) [18–22], ethylene-butadiene rubber (EB) [23], Hydroxyl-terminated polybutadiene (HTPB) [24–27], and styrene butadiene rubber [28]. The crystalline domain of the elastomer or rubber-modified nylon 6 resin is more micronized when the content of the flexible chain segments are increased, resulting in an obvious increase in toughness and a gradual decrease in hardness and strength.

In this paper, the hydroxyl-terminated liquid polybutadiene rubber is used for grafting isocyanate, and the polybutadiene rubber macromolecular activator having acyl-terminated caprolactam is prepared by blocking caprolactam. Then, the rubber-modified nylon 6 is pre-

*Corresponding Author: Hongkai Zhao: School of Materials Science and Engineering, Jilin Jianzhu University, Changchun 130118, China; Email: hkzhao003@126.com
*Corresponding Author: Dengchao Zhang: School of Materials Science and Engineering, Jilin Jianzhu University, Changchun 130118, China; Email: 1054733736@qq.com
Yingshuang Li: School of Materials Science and Engineering, Jilin Jianzhu University, Changchun 130118, China

pared by dissolving the macromolecular activator into the caprolactam monomer. Finally, the morphology and crystallization kinetics of rubber-modified nylon 6 resin are systematically studied.

2 Experiments

2.1 Materials

Caprolactam (industrial grade) was provided by Baoding Mancheng Changsheng Plastic Factory. NaOH (reagent grade) was purchased from Jilin Haodi Chemical Reagent Sales Co., LTD. HDI urea diketone (Desmodur N 3400) with 21.8 wt% content of -NCO was provided by Bayer. Hydroxyl-terminated polybutadiene rubber (industrial grade, HTPB-I) with hydroxyl value of 1.31mmol/g was purcheased from Zibo Qilong Chemical Co., LTD. and its number-average molecular weight (M_n) is 1600-2300. Isopropanol (reagent grade) was provided by Jilin Haodi Chemical Reagent Sales Co., LTD. Toluene (analytically pure) was purchased from Jilin Haodi Chemical Reagent Sales Co., LTD. It was dryed, distilled and purified by 4A molecular sieve before use. Acetone (analytically pure) was purchased from Jilin Haodi Chemical Reagent Sales Co., LTD. Add $KMnO_4$ dropwise to acetone until the liquid turns pink, then place it for 3-4d, following add anhydrous calcium sulfate for dehydration, distilling and purifying. Isopropanol (analytically pure) was provided by Jilin Haodi Chemical Reagent Sales Co., LTD. Bromocresol green indicator: Dissolve 0.1g bromocresol green in 100mL ethanol with the volume fraction of 20%; 0.1mol/L acetone/di-n-butylamine solution: Put 2.60g di-n-butylamine in a 200mL volumetric flask, and add acetone to the scale to dissolve di-n-butylamine, then shake, and store in dark place for future use. Prepare 0.1mol/L HCl standard solution by conventional method.

2.2 Specimen Preparation

Preparation of polybutadiene rubber activator terminated by acyl caprolactam: Put 310g HDI urea diketone and toluene solvent in a 3-mouth flask, slowly add 80g HTPB-I rubber prepolymer, heat to 80°C, and react for 3h until hydroxyl is reacted completely. 113g caprolactam was melt, dried under vacuum to remove moisture, and then add to the above system. The mixed system was reacted at 100°C for 2h, and then heat to 130°C to react until the reaction was completed. The judgment criterion for the end of the reaction is that isocyanate and di-n-butylamine-acetone completely react. Afterwards, add isopropanol solvent to precipitate macromolecule of the rubber grafted acyl caprolactam, place overnight, and wash for several times with isopropanol to remove the small molecular substances. Remove toluene and isopropanol from the obtained product through the reaction flask and finally get acyl caprolactam-terminated HTPB-I activator.

Preparation of rubber copolymerization modification nylon 6: Accurately weigh caprolactam (accounting for 0.8 of the total monomer mass) and rubber activator (accounting for 0.1-0.2 of the total monomer mass), mix uniformly, and remove the trace water by the vacuum at 130°C. Then add NaOH (accounting for 0.008 of the quality of total monomeric substance) catalyst in the remaining caprolactam monoer (accounting for 0.2 of the total monomer mass) and react at 130°C to generate the active anion. Afterwards, mix uniformly, cast at an ordinary pressure, maintain the polymerization reaction for 30 min in the thermal insulation condition of 180°C, and gradually cool and demould to get the product.

Table 1: Mechanical properties of rubber modified nylon resin.

Rubber content (%)	Tensile strength (MPa)	Impact strength (kJ/m^2)	Elongation at break (%)
0.00	65.00	4.30	10.00
5.00	54.00	19.10	63.00
10.00	39.00	45.30	108.00
15.00	21.00	61.50	151.00

As a result of the copolymerization of caprolactam and rubber, the deformation ability of nylon is greatly improved. Increasing the rubber phase content and decreasing the crystallinity both increase toughness and decrease strength.

2.3 Characterization

2.3.1 Infrared spectroscopic (IR) analysis

Polybutadiene rubber and polybutadiene rubber liquid terminated by acyl caprolactam were coated on KBr pellet respectively. Spectrum One infrared spectrometer manufactured by America PE Company is used for analysis. The nylon and rubber-modified nylon were made into thin films by hot pressing. Vertex 70 FTIR of Germany BRUKER Company was used for ATR (attenuated total reflection) infrared analysis, wherein the scan times were 256 times, the resolution was 4cm^{-1}, and the scan range was 500cm^{-1}-4000cm^{-1}.

2.3.2 Wide angle X-ray diffraction (WAXD) analysis

Nylon 6 and rubber-modified nylon 6 were molten for 5 min at 250°C under the protection of nitrogen, and cooled to the room temperature rapidly. The sample was 10mm*10mm*1mm. D8 ADVANCE wide angle X-ray diffraction (WAXD) analysis of Germany BRUKER Company was used for X-ray diffraction analysis of the specimen. The influence of the rubber content on the crystallization behavior of nylon 6 was stydied. Copper target CU-Ka ray (40kV, 200mA, $\lambda = 0.154$nm) was operated. The angle range and scanning speed were 5-40° and 4°/min, respectively.

2.3.3 Scanning electronic microscopy (SEM)

The rubber and modified rubber resin samples were soaked into the liquid nitrogen for brittle failure. The fracture surface was cleaned with acetone and placed into toluene solvent at 120°C for etching for 2h. Scanning electron microscope (SEM, LEO Co., LTD. Germany, model: 1450) was used for observing the dispersion state of the rubber in the matrix after the section was subjected to the gold sputtering.

2.3.4 Differential scanning calorimetry (DSC)

A NETZSCHDSC200PC differential scanning calorimetry was used to study the nonisothermal crystallization behavior of nylon 6 and rubber-modified nylon 6. All samples were heated to 250°C at a heating rate of 20°C/min, subjected to the constant temperature for 10 min, cooled to the room temperature at a cooling rate of 2.5°C/min, 5°C/min, 10°C/min and 20°C/min, respectively, and heated to 250°C at a heating rate of 10°C/min. All DSC curves should be recorded.

3 Results and Discussion

3.1 Representation of prepolymer of the rubber activator and analysis of rubber-modified nylon

Hydroxyl-terminated polybutadiene rubber (HTPB) having high activity, can react with isocyanate without catalyst, and is terminated by caprolactam. Figure 1 shows the infrared analysis of all samples. In Figure 1a of curve spectrum, the absorption peaks at 3080cm^{-1} [29],

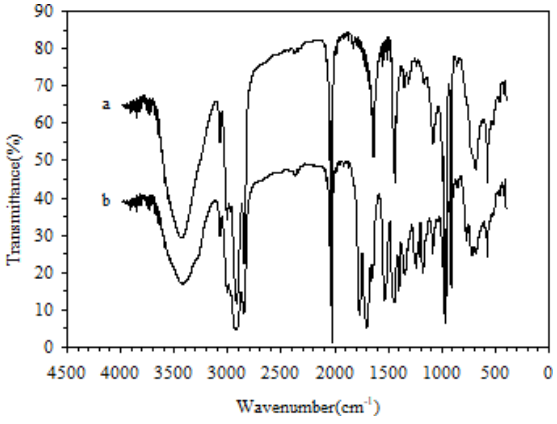

Figure 1: HTPB prepolymer terminated by N-acyl caprolactam and infrared spectroscopy of HTPB prepolymer Note: a: HTPB; b: HTPB terminated by N-acyl caprolactam.

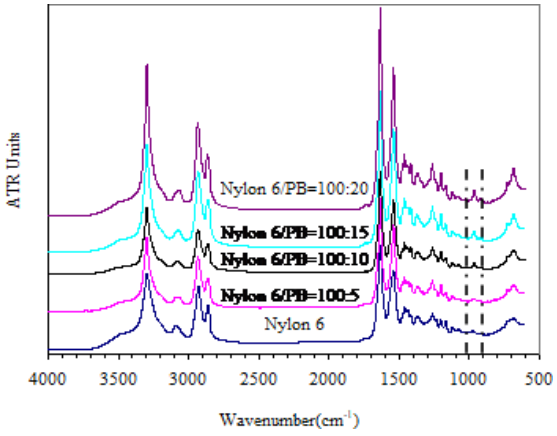

Figure 2: Infrared spectrum of nylon and rubber-modified nylon.

3020cm^{-1}, 1830cm^{-1}, 1641cm^{-1}, 1424cm^{-1}, 1000cm^{-1}, 912cm^{-1}, 690cm^{-1}, and 912cm^{-1} are relatively strong, which suggests that HTPB used in the experiment contains many 1, 2 addition structures [30]. The absorption peaks at 3020cm^{-1} and 970 cm^{-1} (wagging vibration of proton on anti-form olefinic carbon) are relatively strong, which implies that HTPB also contains many anti-form 1, 4 addition structures. The absorption peaks of cis-form 1, 4 addition structure are located at 3020cm^{-1}, 1660cm^{-1}, 1410cm^{-1} and 730cm^{-1}, but the absorption peaks are weak, which suggests that HTPB contains few cis-form 1, 4 addition structures; and 3356cm^{-1} indicates the characteristic spectra of -OH and HTPB [31]. In Figure 1b, the stretching vibration of -NH group is located at 3365cm^{-1} and 1701cm^{-1} [29], and the bending vibration of N-H is located at 1539cm^{-1} [32]. Generally, the stretching vibration absorption of carbonyl of CONH is located at 1768cm^{-1} [30], which is the characteristic spectra of the stretching vibration of NHCO. The characteristic absorption peak of

C=O on tertiary amide is located at 1658cm^{-1} [33], which shows that caprolactam has reacted with -NCO in prepolymer. No absorption peak of -NCO is located at 2270cm^{-1}, suggesting that -NCO has been closed [30]. It shows that HTPB reacts with HDI urea diketone, and caprolactam is used for terminating successfully. Figure 2 shows the infrared spectrum of nylon and rubber-modified nylon. As can be seen from Figure 2, the position of characteristic absorption band of amide group from nylon 6, such as N-H stretching vibration at 3300cm^{-1}, amide absorption band I at 1631cm^{-1}, amide absorption band II at 1536cm^{-1}, amide absorption band III at 1259cm^{-1} [29, 34] and methylene stretching vibration peak at 2931cm^{-1} and 2850cm^{-1} [35], is very obvious. Moreover, one more reflection peak of polybutadiene rubber is provided at 966cm^{-1}, and as the dosage of HTPB is increased, the peak is gradually strengthened, which indicates that active prepolymer generates the copolymer of Nylon 6-HTPB-Nylon 6 by virtue of anionic polymerization.

3.2 Morphology and impact section of rubber-modified nylon

During the polymerization reaction, as the molecular chain of nylon is generated, the microphase separation occurs because the solubility parameter of nylon 6 is diffenent from that of rubber phase. The rubber phase is uniformly distributed in the nylon matrix in situ, which is similar to the two-phase distribution of Styreneic Block Copolymers (SBS). Figure 3 shows the SEM micrographs of cryofracture surfaces after etching. As shown in Figure 3(a), no any change is provided on the surface through the toluene solvent etching. Figure 3(b) shows the section morphology of modified nylon with rubber content of 5%, from which it is found that it is hard to see the etching mark of the rubber phase on the section. This may be because the rubber is very uniformly distributed in the matrix through the covalent bonding, and the content of the rubber phase is too low, so it is insufficient to form the microphase. Figure 3(c) shows the section morphology of the modified nylon with the rubber content of 10%. The etching mark of the rubber phase on the section is very slightly, When the content of the rubber phase is increased, it is too late for part of rubbers to react, or part of rubber cannot be grafted on the active group during rapidly polymerization, resulting to form the microphase. Figure 3(d) shows the section morphology of the modified nylon with the rubber content of 15%. The etching mark of the rubber phase on the section is obviously, and the increase in the rubber phase content makes the size of microphase increase further. Moreover, many etching pits are presented after the toluene etching, but the size is very small and uniform, which indicates that the rubber can form the microphase with uniformly distributed in the matrix. Figure 3(e) presents the section morphology of the modified nylon with the rubber content of 20%. The etching mark of the rubber phase on the section is increasingly obvious, and the size is increased and nonuniform, which indicates that the content of the rubber failing to participate in the polymerization is further increased, and the big microphase is formed, so they cannot be distributed in the matrix uniformly.

The roughness of the impact section can reflect the situation of crack propagation of nylon 6 and modified nylon 6. Figure 4 shows the SEM micrographs of impact section of nylon 6 and rubber-modified nylon 6. It can be seen from Figure 4 that the molecular chain of the pure nylon 6 is relatively structured and has relatively high crystallinity. The energy cannot be consumed timely under the impact of external forces, and the craze is produced and rapidly expanded into the big crack, then, the resin is fractured soon and shows brittle. Therefore, the impact section is relatively smooth. When the rubber content in the resin is increased, the impact section is much rough comparing with the that of pure nylon 6. Especially, when the rubber content is higher than 15%, the resin shows obvious ductile fracture. Therefore, it can be concluded that the molecular chain can be loose and is subjected to the shear yield under the effect o the external force, so that the impact energy is dissipated.

3.3 Crystalline structure of the rubber-modified nylon

Nylon 6 is the polycrystalline crystalline polymer, and takes on α and γ crystal structures according to the different crystallization conditions. α is the relatively common crystal form, in which the molecular chain in the crystalline region is completely stretched. Amide chain segment and methylene chain segment are located in the same plane, and are connected to each other through hydrogen bond. As a result, the plane slice layer is formed, which is generally generated in the high crystallization temperature. γ crystal form is metastable, in which the hydrogen bond direction is close to the plane of the vertical framework, which shows the kilted slice layer. γ crystal form generally generated in the low temperature. X-ray diffraction of α crystal form has two peaks near 20.5° and 23.6°, which belongs to the (200) and (002) crystal faces of α crystal form, respectively. γ crystal form only has the single peak at 2θ = 21.5°, which belongs to the (200)

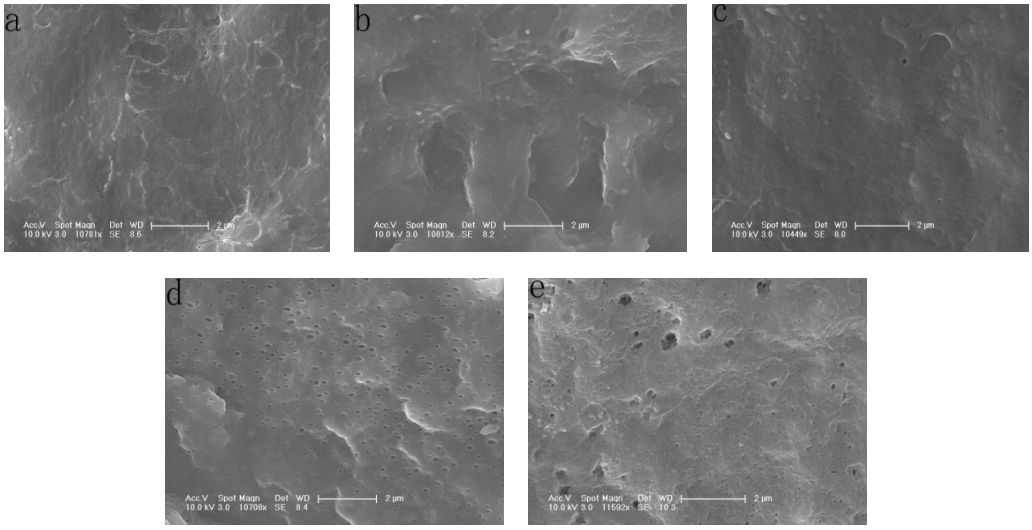

Figure 3: SEM micrographs of cryofracture surfaces after etching: a: Nylon 6; b: Nylon 6/HTPB=100/5; c: Nylon 6/HTPB=100/10; d: Nylon 6/HTPB=100/15; e: Nylon 6/HTPB=100/20.

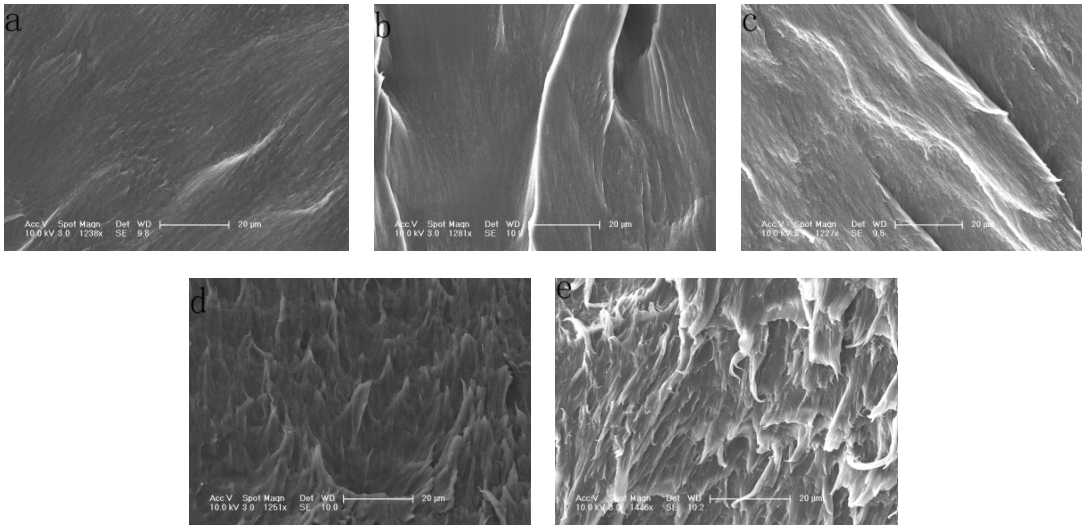

a: Nylon 6; b: Nylon 6/HTPB=100/5; c: Nylon 6/HTPB=100/10: d: Nylon 6/HTPB=100/15; e: Nylon 6/HTPB=100/20.

Figure 4: SEM micrographs of impact section of nylon 6 and rubber-modified nylon 6.

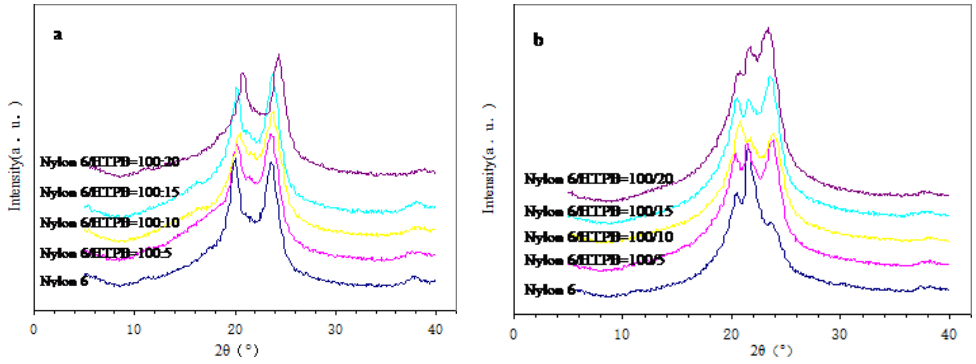

a: slice analysis after anionic polymerization; b: quick-cooling tabletting analysis after melting for 5min at 250°C.

Figure 5: WAXD spectrogram of nylon 6 and rubber-modified nylon 6.

and (101) crystal faces of γ crystal form. Figure 5a shows the WAXD spectrogram of nylon 6 pellets polymerized and modified by liquid rubber with different contents in situ. It can be seen that two peaks of α crystal form are presented near 20.5° and 23.6°, and no new diffraction peak is found, which suggests that the introduction of the rubber prepolymer does not change the crystalline structure of the nylon 6 after the polymerization at high temperature. Furthermore, the position of the diffraction angle of α crystal form of nylon 6 is not basically changed when the liquid rubber content is in the range of 0-15%, and when the rubber content is up to 20%, the spectral peak of crystal face (002+202 and 200) moves towards the high angle. The reason may be that the interplanar spacing of the molecular chain of nylon 6 is reduced due to the orientation shrinkage of rubber occurs, and the strength of the diffraction peak of α crystal form is decreased caused by the mixing of the rubber. Therefore, the addition of the rubber affect the formation of α crystal form. In general, the rubber has big influence on the crystal form of nylon 6, thereby, keeping the original nature of nylon 6 is important. Figure 5b shows the WAXD spectrogram of nylon 6 pellets polymerized and modified by liquid rubber with different contents in situ after melting in high temperature and quick-cooling. It can be seen that many γ crystal forms are provided on the molecular chain of nylon 6 when quick-cooling, which indicates that it is too late for the molecular chain to arrange in order, thus, forming the metastable crystal form. As the rubber content is increased, the diffraction peak of α crystal form is obviously enhanced, indicating that the crystal form of nylon 6 changes from strong γ crystal to crystals with γ and α crystal form coexisting, and then changed to strong α crystal form. These results suggest that the activity ability of the molecular chain becomes strong due to the existence of the flexible chain segment of the rubber, and the molecular chain can be arranged in order in shorter time, resulting in the formation of the relatively stable α crystal.

3.4 Nonisothermal crystallization kinetics

The crystallization properties of nylon 6 and rubber-modified nylon 6 resin are different as the processing temperature is different. This paper studied the nonisothermal crystallization kinetics by virtue of Jeriorny method [36]. Figure 6 gives the DSC curve of nylon 6 and modified nylon 6 in the nonisothermal crystallization process. It can be seen that the temperature for starting crystallization gradually shifts towards the lower temperature, and the crystallization peak broadens obviously as the cooling rate is increased. Because the cooling rate is increased, the chain segment is crystallized at the lower temperature, and the activity ability of the chain segment decreases. Therefore, only part of chain segments can enter the crystalline phase and become the most stable crystal. As the cooling rate is increased, the degree of crystal imperfection increases, so the crystallization temperature range increases and the crystallization peak become wider. The temperature for starting crystallization of the rubber-modified nylon 6 moves to the low temperature, suggesting that the nylon 6 chain segment enters the unit cell, reducing the nucleation due to the flexible rubber chain segment.

Figure 7 shows the DSC heating curves of nylon 6 and rubber-modified nylon 6. It can be seen from Figure 7(a) that the melting point temperature (T_m) of nylon 6 subjected to the anionic polymerization is 211.00°C, and the T_m of the modified nylon presents the decreases as the liquid rubber activator is added. For example, the T_m of modified nylon 6 with the rubber content of 20% is 202.67°C. It can be seen that the rubber molecules increase the flexibility of nylon chain, and also reduce the hydrogen bond density of nylon 6. At the same time, the proportion of the amorphous region is increased, leading to the limitation and interference of the growth of spherulites. Therefore, the growth of spherulite of the polymer is reduced. It can be seen from Figure 7(b) that nylon 6 and modified nylon 6 can crystallize at cooling rate of 10°C/min. Because in the follwing second heating curves, the melting peak of the crystal appeare. It can be seen that the T_ms of nylon 6 and modified nylon 6 slightly increase, which indicates that the chain segment has sufficient time to arrange into the stable state when cooling.

The calculation formula (1) of the relative crystallinity *X(T)* in the nonisothermal crystallization process is as follows [37]:

$$X(T) = \frac{\int_0^T \frac{dH_c}{dT} dT}{\int_0^\infty \frac{dH_c}{dT} dT} \quad (1)$$

where *X(T)* is the relative crystallinity when the temperature is *T*, and dH_c/dT is the heat flow rate of crystallization at *T*.

Figure 8 shows the curves of relative crystallinity against time for all the resin. It can be seen that the curves are obvious S type. When the relative crystallinity is within 10%, the nonisothermal crystallization of polymer starts, and the nucleation rate is very small. At this time, the crystallization rate is controlled by the nucleation process, and the change in the relative crystallinity with temperature or time is slower. As the nucleation rate becomes faster, the crystal growth becomes quickly, the crystallization rate increases rapidly, and the relative crystallinity changes faster with time or temperature. When the rela-

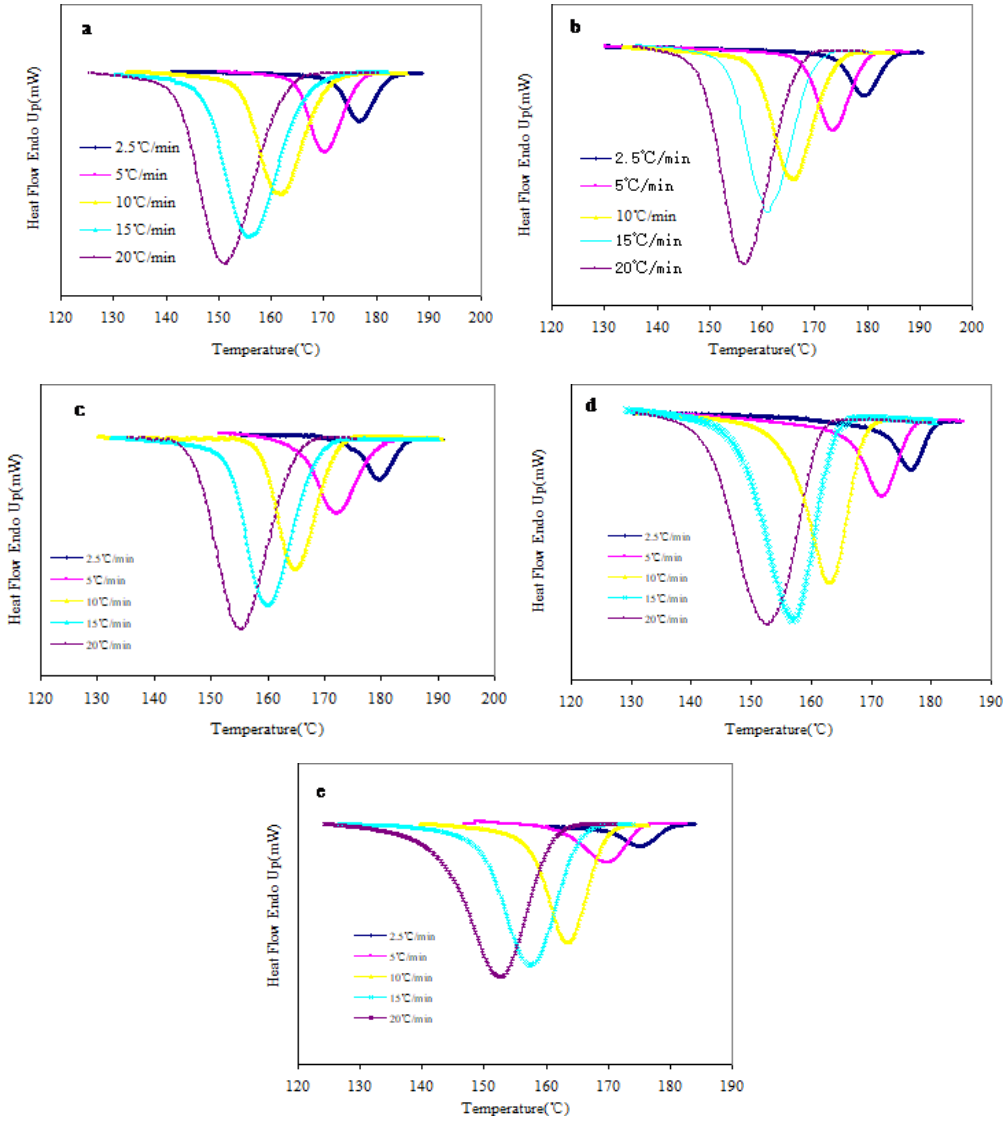

Nylon 6; b: Nylon 6/HTPB=100/5; c: Nylon 6/HTPB=100/10; d: Nylon 6/HTPB=100/15; e: Nylon 6/HTPB=100/20.

Figure 6: DSC curve of nonisothermal crystallization of nylon 6 and rubber-modified nylon 6.

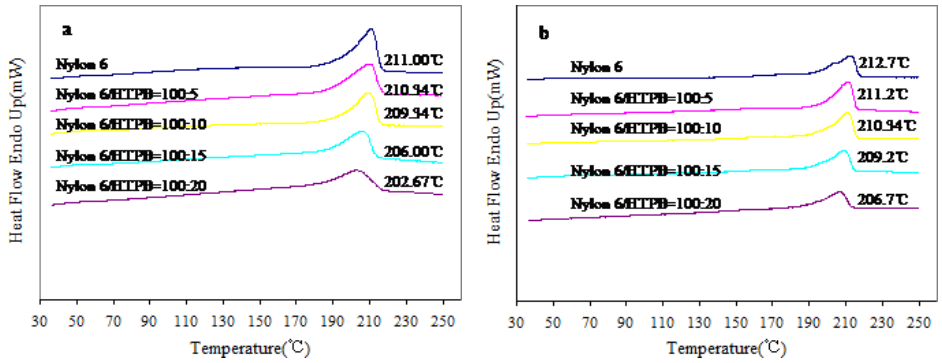

a: heating after anionic polymerization and slicing; b. cooling and heating at constant speed after melting for 5min at 250°C.

Figure 7: DSC heating curves of nylon 6 and rubber-modified nylon 6.

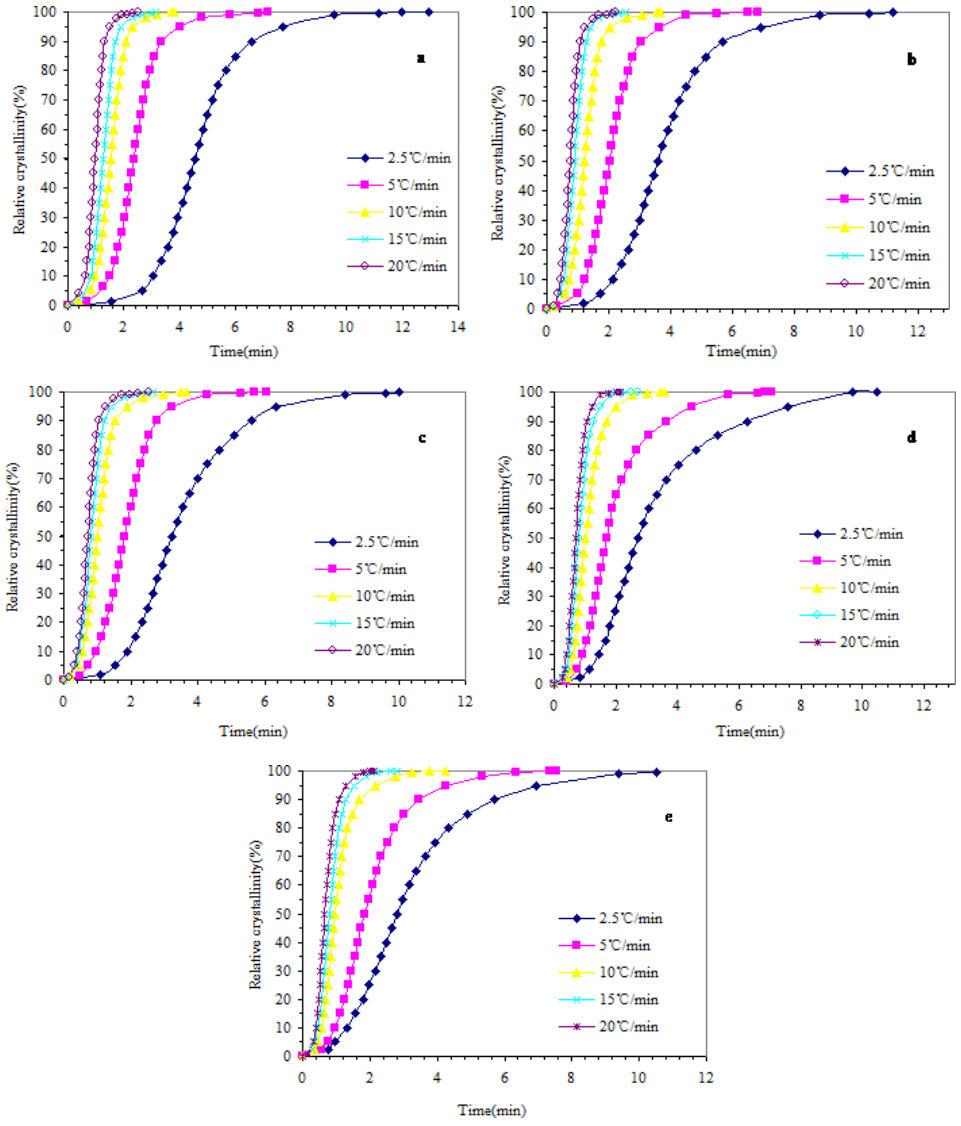

a: Nylon 6; b: Nylon 6/HTPB=100/5; c: Nylon 6/HTPB=100/10; d: Nylon 6/HTPB=100/15; e: Nylon 6/HTPB=100/20.

Figure 8: Plots of the relative crystallinity with crystallization time.

tive crystallinity is above 90%, the nucleation rate of the crystal is still large, but the crystal growth rate gradually becomes slow, resulting in a slower change of the relative crystallinity with temperature and time.

In the nonisothermal process, the time-temperature transformation will be carried out by using the formula:

$$t = (T_0 - T)/R \tag{2}$$

where t is the crystallization time, T_0 is the initial crystallization temperature, T is the crystallization temperature, and R is cooling rate. The relation curve of $X(t)$ and t can be obtained from the time-temperature transformation, and the half-crystallization time $t_{1/2}$ can be directly calculated from the curve. The DSC crystallization curve of varying temperature at constant rate can be taken as the isothermal crystallization process. Therefore, the relevant parameters can be corrected, and Avrami equation is popularized and applied to the nonisothermal crystallization process. In other words, Avrami equation can be expressed as Formula (3) [38, 39].

$$\lg\left[-\ln\left(1 - X(t)\right)\right] = \lg Z_t + n\lg t \tag{3}$$

where n is Avrami index, which is related to the nucleation mechanism and growth mode of the crystal, and Z_t is the rate parameter in the nonisothermal crystallization process. Jeziorny proposes that the rate parameter Z_t should be corrected, so that Avrami equation can be applicable to describe the nonisothermal crystallization pro-

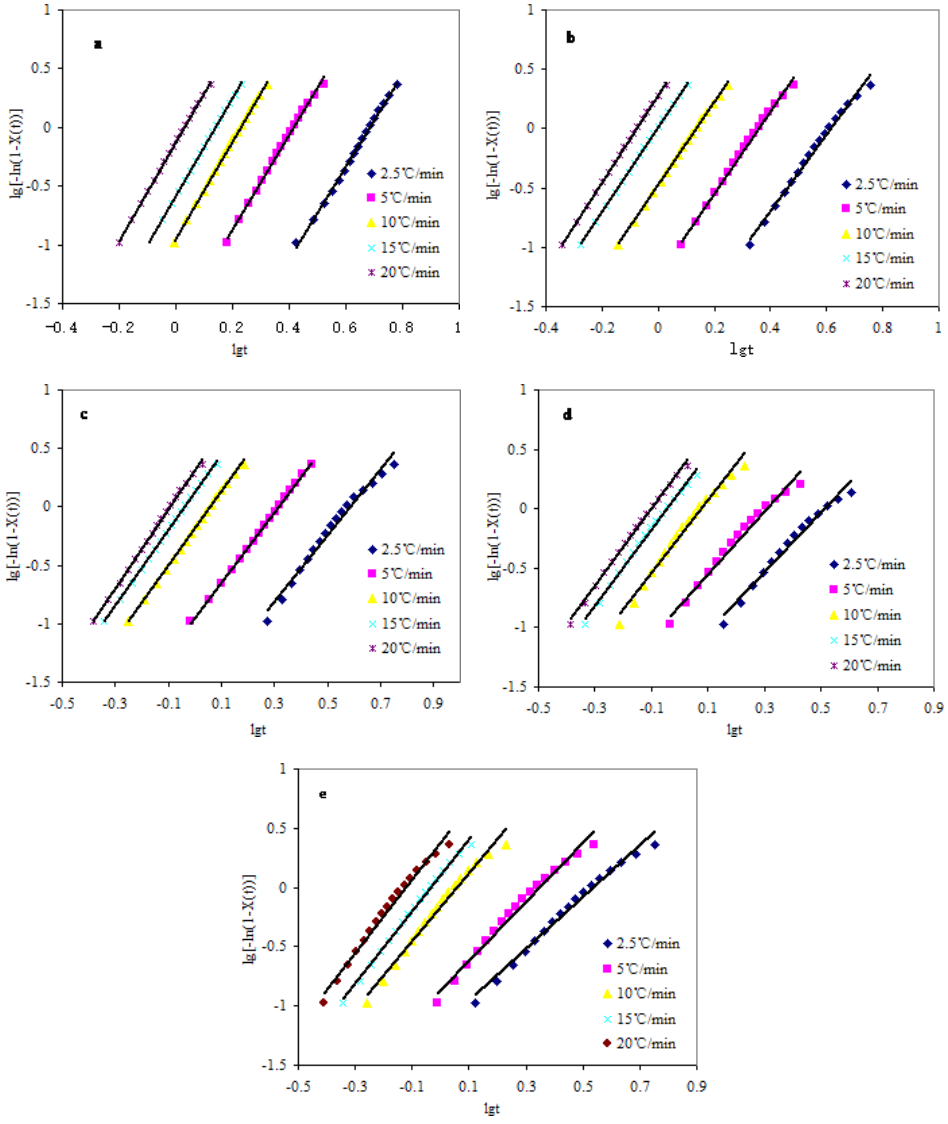

a: Nylon 6; b: Nylon 6/HTPB=100/5; c: Nylon 6/HTPB=100/10; d: Nylon 6/HTPB=100/15; e: Nylon 6/HTPB=100/20.

Figure 9: Avrami plots of nylon 6 and rubber-modified nylon 6.

cess, namely, Formula (4) [36]:

$$\lg Z_c = \frac{\lg Z_t}{\Phi} \tag{4}$$

where Z_c is the rate constant after correction; and φ is the heating or cooling rate.

The crystallization kinetics curves of samples are obtained by plotting $\lg[-\ln(1-X_t)]$ against $\lg t$ and are shown in Figure 9. It can be seen from Figure 9 that $\lg[-\ln(1-X_t)]$ has good linear relation with $\lg t$ under different cooling rates when the relative crystallinity is 10%-90%. n and Z_c are calculated from the slope and intercept of the fitting curves and are listed in Table 2. It can be seen from Figure 9 and Table 2 that n value of nylon 6 is 3.97-4.22, suggesting that nylon 6 crystal grows mainly in a three-dimensionally during the nonisothermal crystallization process. n value of rubber-modified nylon 6 is 2.19-3.65, indicating that its growth mode is the coexistence of the two-dimensional discoid growth and three-dimensional spherulitic growth. In addition, a certain deviation is provided when entering the late period of the crystallization. This is because the crystalline grains are contacted to each other, and the crystal stops growing in the contact direction, while the crystal continues to grow in the direction without collision, resulting in the imprvement of the incomplete part. in the early stage of crystallization, the crystallization rate is controlled by nucleation, and the crystal growth rate changes with the time. In the late stage of crys-

Table 2: Characteristic parameters of nylon 6 and rubber-modified nylon 6 in the nonisothermal crystallization process.

Sample	Cooling rate (°C/min)	T_S	T_{max}	T_F	ΔHc/J·g^{-1}	n	Z_c	$t_{1/2}$ (min)
PA6	2.50	188.78	176.87	155.59	55.40	3.97	0.08	4.54
	5.00	180.65	170.32	146.32	54.32	4.02	0.46	2.36
	10.00	177.13	161.97	138.99	53.35	4.14	0.80	1.54
	15.00	171.44	155.69	128.19	53.58	4.18	0.91	1.26
	20.00	170.93	151.27	120.23	51.51	4.22	0.99	0.98
HTPB-5%	2.50	187.53	179.41	158.17	57.62	3.23	0.16	3.59
	5.00	183.48	173.65	149.33	57.25	3.46	0.56	2.03
	10.00	177.97	165.80	140.93	57.47	3.50	0.90	1.23
	15.00	174.01	160.94	136.19	53.08	3.60	1.00	0.89
	20.00	169.27	156.60	127.13	54.59	3.65	1.03	0.76
HTPB-10%	2.50	185.62	179.62	160.54	50.73	2.84	0.22	3.24
	5.00	180.40	172.23	151.06	51.34	3.01	0.65	1.83
	10.00	176.30	164.80	137.48	52.62	3.15	0.97	1.02
	15.00	172.94	160.19	132.52	50.86	3.26	1.02	0.81
	20.00	170.27	155.27	118.29	50.80	3.38	1.04	0.72
HTPB-15%	2.50	182.16	176.53	150.41	45.89	2.53	0.30	2.70
	5.00	179.15	172.82	144.38	41.54	2.64	0.69	1.70
	10.00	172.40	163.13	136.40	46.20	3.08	0.95	1.02
	15.00	168.19	156.94	127.13	45.02	3.20	1.02	0.79
	20.00	165.27	152.60	123.04	44.26	3.25	1.04	0.70
HTPB-20%	2.50	181.28	175.12	153.43	27.76	2.19	0.34	2.69
	5.00	177.73	169.82	140.07	30.09	2.47	0.69	1.69
	10.00	172.57	163.47	130.58	42.05	2.89	0.96	0.97
	15.00	169.08	157.44	126.92	38.92	3.08	1.02	0.78
	20.00	166.27	152.60	117.00	37.39	3.11	1.04	0.65

T_S represents the temperature for starting crystallization; T_{max} represents the crystallization temperature at the peak position; and T_F represents the temperature for ending crystallization.

tallization, the crystallization process is controlled by diffusion, and the growth rate becomes slower.

The nonisothermal crystallization parameters of the nylon and modified nylon at different cooling rates are listed in Table 2. It can be seen from Table 2 that the temperature at which crystallization starts (T_S) and crystallization peak temperature (T_{max}) of the rubber-modified nylon 6 and nylon 6 both move to a low temperature direction as the cooling rate continuously increases, suggesting that the nonisothermal crystallization process of the nylon is controlled by nucleating. At a low cooling rate, the chain segment has sufficient time to arrange into the stable state and further nucleate to form the microphase. When the cooling rate is continuously increased, the time for chain segment stacking becomes shorter, so, it is difficult to enter the unit cell with the stable state, resulting in delayed nucleation and a decrease in initial crystallization temperature. The half-crystallization time ($t_{1/2}$) becomes shorter as the cooling rate is increased, which indicates that the nucleation rate increases due to shortened crystallization time caused by cooling. On the other hand, the $t_{1/2}$ decreases as the rubber content is increased, suggesting that the rubber promotes the crystallization of the nylon 6, and accelerates the crystallization rate. As the cooling rate is increased, the crystallization rate constant Z_c of nylon 6 increases, and $t_{1/2}$ obviously shortened. This is because that the increase in cooling rate increases the degree of supercooling and accelerates the transition of the system from the melt state to the crystalline state, thus increasing the crystallization rate. As the rubber content is increased, the $t_{1/2}$ of rubber-modified nylon 6 is shortened at the same cooling rate, indicating that the addition of the rubber promotes the crystallization of nylon 6 matrix.

4 Conclusion

The rubber activator terminated by acyl caprolactam was prepared by grafting the prepolymer of hydroxyl-terminated polybutadiene rubber with HDI urea diketone and then terminating with caprolactam. The liquid rubber-modified nylon 6 resin was prepared by anionic polymerization, where rubber activator (<20wt%) and caprolactam monomer underwent a polymerization reaction, and sodium hydroxide acted as a catalyst. The analysis of section morphology of nylon 6 suggested that when the content of rubber was less than 5wt%, the nylon 6 showed brittle fracture. When the content of rubber was more than 15wt%, the resin showed an obvious ductile fracture. On the other hand, when the rubber activator content was less than 10wt%, almost all rubber activators could participate in the polymerization, and the microphase separation was not obvious. When the rubber activator was more than 15wt%, only part of rubber activators can participate in the polymerization. The WAXD spectrogram of samples indicated that the liquid rubber did not change the structure of α crystal at high polymerizaito temperature, The analysis of nonisothermal crystallization kinetics of nylon 6 and rubber-modified nylon 6 suggested that the nucleation rate of chain segment of nylon 6 became slower due to the flexile rubber chain segment. The change in n value showed that the nylon 6 crystals grew in three-dimensionally, and rubber-modified nylon 6 crystals grew in the coexistence of the two-dimensional discoid growth and three-dimensional spherulitic growth. Finally, the addition of rubber facilitated the crystallization of nylon 6 matrix.

Acknowledgement: The authors would like to thank the funding provided by the Jilin Provincial Development and Reform Commission Industrial Technology Research and Development Project (No. 2020C027-4), And Jilin Province University Student Innovation and Entrepreneurship Training Program (Project No. 8570036504).

References

[1] Martuscelli E, Riva F, Sellitti C. Crystallization, morphology, structure and thermal behaviour of nylon-6/rubber blends. *Polymer*. 1985, 26, 270-282.

[2] Cimmino S, Coppola F, D'Orazio L. Greco R. Ternary nylon-6/rubber/modified rubber blends: Effect of the mixing procedure on morphology, mechanical and impact properties. *Polymer*. 1986, 27,1874-1884.

[3] Borggreve RJM, Gaymans RJ, Schuijer J. Brittle-tough transition in nylon-rubber blends: effect of rubber concentration and particle size. *Polymer*. 1987, 28,1489-1496.

[4] Dijkstra K, Laak JT, Gaymans RJ. Nylon-6/rubber blends: 6. Notched tensile impact testing of nylon-6(ethylene-propylene rubber) blends. Polymer. 1994, 35,315-322.

[5] Oommen Z, Zachariah SR, Thomas SJ. Melt Rheology and Morphology of Uncompatibilized and In Situ Compatibilized Nylon-6/Ethylene Propylene Rubber Blends. *Appl. Polym. Sci*. 2004, 92, 252-264.

[6] Kayano Y, Keskkula H, Paul DR. Evaluation of the fracture behaviour of nylon 6/SEBS-g-MA blends. *Polymer*.1997, 38, 1885-1902.

[7] Jha A, Bhowmick AK. Thermal degradation and ageing behaviour of novel thermoplastic elastomeric nylon-6/acrylate rubber reactive blends. *Polym. Degrad. Stab*. 1998, 62, 575-586.

[8] Veith CA, Cohen RE, Argon AS. Morphologies of poly (dimethylsiloxane)-nylon-6 diblock copolymers and blends. *Polymer*.1991, 32,1545-1554.

[9] Fang X, Hutcheon R, Scola DA. Microwave syntheses of poly(ϵ-caprolactam-co-ϵ-caprolactone). *J. Polym. Sci. Part A Polym. Chem*. 2000, 38,1379–1390.

[10] Michell RM, Muller AJ, Castelletto V. Effect of sequence distribution on the morphology, crystallization, melting, and biodegradation of poly(epsilon-caprolactone-co-epsilon-caprolactam) copolymers. *Macromolecules*. 2009, 42, 6671-6681.

[11] Ruppert M, Landfester K, Ziener U. Anionic polymerization of cyclic ester and amide in miniemulsion: Synthesis and characterization of poly(ϵ-caprolactone) and poly(ϵ-caprolactone-co-ϵ-caprolactam) nanoparticles. *J. Polym. Sci., Part A Polym. Chem*. 2010, 48, 4929-4937.

[12] Gardlund ZG. Bator MA. In situ polymerization of nylon–polyurea block copolymers. I. Synthesis and characterization. *J. Polym. Sci. Polym. Chem. Edi*. 1990, 40, 2027-2035.

[13] Yeh JL, Kuo JF, Chen CY. Morphology and properties of nylon 6-polyoxypropylene-nylon 6 block copolymers. *Mater. Chem. Phys*. 1994, 37, 161-169.

[14] Pandya MV, Subramaniyam M, Desai MR. Synthesis and characterization of nylon 6 triblock copolymer using new hybrid soft segment. *Eur. Polym. J*. 1997, 33, 789-794.

[15] Kim KJ, Hong DS, Tripathy AR. Toughening and phase separation behavior of nylon 6–PEG block copolymers and in situ nylon 6–PEG blend via in situ anionic polymerization. *J. Appl. Polym. Sci*. 1999, 73, 1285-1303.

[16] Petrov P, Gancheva V, Philipova T. Synthesis of nylontriblock copolymers with bifunctional polymeric activators. *J. Polym. Sci., Part A: Polym. Chem*. 2000, 38, 4154-4164.

[17] Tsui SW, Johnson AF. Thermal behaviour of nylon 6-poly (ether-esteramide) block copolymers. *J. Mater. Sci*. 1995, 30, 5967-5972.

[18] Yn MS, Ma CCM. Poly(ϵ-caprolactam)-poly(butadiene-co-acrylonitrile) block copolymers. I. Synthesis, characterization, mechanical properties, and morphology. *J. Appl. Polym. Sci*. 1994, 53, 213-224.

[19] Yn MS, Ma CCM, Lin SH. Pultrusion of poly(ϵ-caprolactam)/poly(butadiene-co-acrylonitrile) composites: I. Simulation and a mathematical model. *Compos. Sci. Technol*. 1995, 54, 123-131.

[20] Ma CCM, Yn MS. Poly (ϵ-caprolactam)-poly (butadiene-co-acrylonitrile) block copolymers II. Processability and properties of pultruded glass-fiber-reinforced composites. *Mater. Chem. Phy*. 1995, 42, 17-24.

[21] Stehlícek J, Lednicky F, Baldrian J. On the synthesis of poly(ϵ-caprolactam)-poly(butadiene-co-acrylonitrile) block copolymers for the reaction injection molding process. *Polym. Eng. Sci.* 1991, 31, 422-431.

[22] Pandya MV, Subramaniyam M, Desai MR. Synthesis and characterization of nylon 6 triblock copolymer using new hybrid soft segment. *Eur. Polym. J.* 1997, 33, 789-794.

[23] Omonov TS, Harrats C, Moussaif N, Groeninckx G, Sadykov SG, Ashurov NR. Polyamide 6/ethylene-butylene elastomer blends generated via anionic polymerization of ϵ-caprolactam: Phase morphology and dynamic mechanical behavior. *J. Appl. Polym. Sci.* 2004, 94, 2538-2544.

[24] Petrov P, Jankova K, Mateva R. Polyamide-6-b-polybutadiene block copolymers: Synthesis and properties. *J. Appl. Polym. Sci.* 2003, 89, 711-717.

[25] Harrats C, Fayt R, Jerome R. Effect of block copolymers of various molecular architecture on the phase morphology and tensile properties of LDPE rich (LDPE/PS) blends. Polymer. 2002, 43, 5347-5354.

[26] Roman S, Srubar R, Jan R. Polymerization of lactams, 88. Copolymers poly(ϵ-caprolactam)-block-polybutadiene prepared by anionic polymerization, part III. Model polymerizations initiated with potassium salt of ϵ-caprolactam and accelerated with isocyanates and their derivatives. *Macromol. Chem. Phys.* 2010, 198, 1147-1163.

[27] Stehlicek J, Hauer J, Puffr R. Block copolymers of 6-hexanelactam and 12-dodecanelactam. *Polymer*. 1996, 37, 2533-2540.

[28] Allen WT, Eaves DE. Caprolactam based block copolymers using polymeric activators. *Macromol. Mater. Eng.* 1977, 58, 321-343.

[29] Jiang L, Marcus RK.Microwave-assisted, grafting polymerization preparation of strong cation exchange nylon 6 capillary-channeled polymer fibers and their chromatographic properties. *Anal. Chim. Acta.* 2017, 997, 52-64.

[30] Chen GJ, Tang KL, Niu GR. Synthesis and characterization of the novel nylon 12 6 based on 1,12-diaminododecane. *Polym. Eng. Sci.* 2019, 59, 192-197.

[31] Fazullina DD, Mavrina GV, Shaikhievb IG, Nizameevc IR. Ultrafiltration of Oil-in-Water Emulsions with a Dynamic Nylon-Polystyrene Membrane. *Petrol. Chem.* 2018, 58, 145-151.

[32] Sucharitpong T, Lam NT, Sukyai P. Production of Nylon-6/Cellulose Nanocrystal Composite Films Using Solvent Dissolution. *Sugar.Tech.* 2019.

[33] Huang YQ, Wu JW, Li G. Oxygen barrier, free volume, and blending properties of polyamide 12/poly (vinyl alcohol) blends. *Polym. Adv. Technol.* 2018, 29, 1649-1660.

[34] Roy S, Tang XZ, Das T. Enhanced Molecular Level Dispersion and Interface Bonding at Low loading of Modified Graphene Oxide to Fabricate Super Nylon 12 Composites. *ACS Appl. Mater. Inter.* 2015, 7, 3142-3151.

[35] Munirajappa ML, Basavaraju RH. Microstructural characterization of short glass fiber and PAN based carbon fiber reinforced nylon 6 polymer composites. *Polym. Eng. Sci.* 2018, 58, 1428-1437.

[36] Jeziorny A. Parameters characterizing the kinetics of the non-isothermal crystallization of poly(ethylene terephthalate) determined by d.s.c. *Polymer.* 1978, 19, 1142-1144.

[37] Kim SH, Ahn SH, Hirai T. Crystallization kinetics and nucleation activity of silica nanoparticle-filled poly(ethylene 2,6-naphthalate). *Polymer*. 2003, 44, 5625-5634.

[38] Avrami MJ. Kinetics of phase change. *Chem. Phys*. 1939, 7, 1103-1112.

[39] Avrami MJ. Kinetics of Phase Change 2. *Chem. Phys*. 1940, 8, 212-224.